Nonlinear Behaviour of a Skew Slab Bridge under Traffic Loads

[1]L.A. Abozaid, [2]Ahmed Hassan, [3]A.Y. Abouelezz and [3]L.M. Abdel- Hafez

[1]Department of Civil Engineering, High Institute of Engineering & Technology, El- Mania, Egypt
[2]Department of Civil Engineering, Faculty of Engineering, Beni-Suef University, Egypt
[3]Department of Civil Engineering, Faculty of Engineering, El-Minia University, Egypt

Abstract: This paper presents a comparison between certain results of previous experimental studies and the nonlinear finite element analysis of a reinforced concrete skew slab. The primary parameters studied were the skew angle and the steel arrangements. The slabs were designed using an elastic stress field under an ultimate design load as an input to the direct design method. A good agreement between the experimental and theoretical results was obtained. Furthermore, a theoretical study was performed on an actual ribbed bridge consisting of two lanes under the effect of traffic loads based on Egyptian code of practice recommendations. The parameter investigated in this analytical study was the skew angle, which was varied from 0° to 45°. Skew angles of 0° and 30° were used to study the effect of concrete grade on the overall behaviour of bridge decks. Compressive strength values of 400, 500, 600, 700, 800 and 900 kg/cm² were considered for each skew angle. In the theoretical study, the skew angle and concrete grade had a significant influence on the overall behaviour of the slab.

Key words: Bridge · Nonlinear analysis · Skew slab · Standard traffic load

INTRODUCTION

Skew bridges can be found on highways, river crossings and other extreme grade fluctuations where skewed geometry is necessary because of space limitations. The skew bridge is used to increase high speeds and provide additional safety requirements for modern traffic so that the connection of highways with bridges can be as continuous as possible. In practice, reinforced concrete bridge slabs are designed using various methods based on both linear elastic and plastic theories. Elastic and yield load theories cannot be used for complex structures with complicated loading and boundary conditions. For many structures, the primary sources of material nonlinearity are the cracking load, crushing in the concrete through the depth and yielding of the reinforcing steel [1]. The difficulty in analytically modelling the complex behaviour of reinforced concrete in its nonlinear zone is well known. This complexity has led engineers to previously rely largely on empirical formulas, which were derived from numerous experiments for the design of reinforced concrete structures. The finite

element method makes it feasible to consider a non-linear response [2]. The success of the analysis depends on several factors, including appropriate modelling of the composite material behaviour [1]. Several material models [3-6] have been proposed to predict the response of concrete. However, they include a large number of function and material parameters and involve tedious programming and computational effort. The increasing demand for high skew bridges has been accompanied by the development of computer-aided methods of analysis and it is now generally possible to analyse and design a structure at any skew angle [7, 8]. The inclination of the centre line of traffic to the normal of the centre line of the river (in the case of a river bridge) or other corresponding obstruction is called the skew angle, as shown in Fig. 1. The analysis and design of a skew bridge is much more complicated compared to that for a straight bridge. In the skew bridge, the span length, deck area and pier length increase proportionally to cosec ?, where ? is the skew angle [9]. The presence of skew in a bridge causes the analysis and design of bridge decks to be intricate [10]. The force flow in skew bridges is much more complicated

---

Corresponding Author: Ahmed Hassan, Civil Engineering Department, Faculty of Engineering, Beni-Suef University, Egypt.
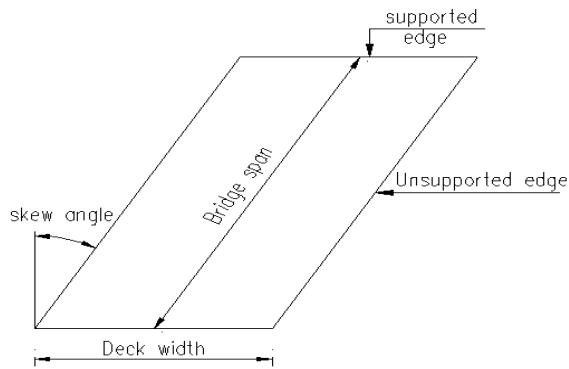
Fig. 1: Plan of skew deck slab.

compared to that in straight-angle bridges. Analytical calculations alone do not provide sufficient accuracy for structural design. A numerical analysis needs to be performed in which a skew bridge can be modelled in several ways with different degrees of sophistication [11]. The finite element analysis results obtained for a skewed bridge [12] indicate that the maximum live load bending moments and deflections in the T-beams decrease for skewed bridges, while the maximum shear, torsion and support reactions in the T-beams increase for skewed bridges for all considered span lengths (12, 16, 20 and 24 m) compared to those for a straight bridge.

The objective of this work is to present the typical experimental and nonlinear finite element analysis results for slabs designed using the direct design method. Furthermore, this report will theoretically study the behaviour of a two-lane, simply supported ribbed bridge under the effect of traffic loads case number one, which is recommended by the Egyptian code of practice. Three different skew angles (15°, 30° and 45°) were studied. The skewed bridges' results were compared with those of straight bridges (skew angle = 0°). The second parameter was the effect of the concrete grade; six types of reinforced concrete with strengths of 400, 500, 600, 700, 800 and 900 kg/cm^2 were used in the bridge decks. These models have been analysed within these parameters for skew angles of 0° and 30°.

Finite-Element Analysis Methodology: The theoretical study was performed using the well-known structural software ANSYS, which is based on the finite element method. The solid65 element is used in ANSYS to model the concrete element. This element is defined by eight nodes with three degrees of freedom at each node: translations in the nodal x, y and z directions. The most important aspect of this element is its treatment of

nonlinear material. The element is capable of simulating plastic deformations, cracking in three orthogonal directions and crushing. The link8 element is used in ANSYS to model the steel reinforcement. Two nodes are required for this element. Each node has three degrees of freedom: translations in the nodal x, y and z directions. The link 8 element is a uniaxial tension-compression element. Similar to a pin-jointed structure, no bending of the element is considered. The reinforcing steel elements are connected to the concrete elements at the nodal points. The composite behaviour is enforced through compatibility at the nodes. A large number of elements were used in this analysis to satisfy the details of steel reinforcements (44880 solid65 elements as concrete and 26321 link8 elements as steel reinforcement). Coarse increments were used in certain stages of loading and finer increments were used in the cracking stage and close to failure. The finer increments were used to ensure that cracking and failure loads could be predicted within 2% because failure was expected within that range. In this analysis, the convergence tolerance was taken at 0.001 of displacement, with a maximum iteration number of 22, to reduce the accumulation forces within the iteration.

Verification Using Computer Software (Ansys): The experimental program [15] consisted of testing six skew slabs; three slabs were used to verify the results and are presented in Table 1. The slabs were simply supported on the two parallel shorter edges and the parallel longer edges were left free. Models one to five had a rectangular cross section and a slab thickness of 100 mm. Model three was a ribbed slab in which only the longitudinal ribs were simply supported. Full details of the tested models (steel reinforcement, loading system and boundary condition) can be found by El-Hafez [15]. The measured and assumed material properties used in this analysis are provided in Table 2.

Analysis and Comparisons: Table 3 summarises the comparison between the experimental and the theoretical results for all studied models. Figs 2-4 present comparisons between the experimental and the theoretical results for load-deflection and Figs 5-7 present the difference between the experimental and theoretical load-longitudinal steel strain curves. This comparison indicates that the theoretical cracking load was 1.00 and 0.99 of the experimental load for models 1 and 3, respectively; the theoretical cracking load was 0.80 of the experiment load for model 2, which may be due to an error in the experiment. The theoretical yield load was 1.00, 0.92 and
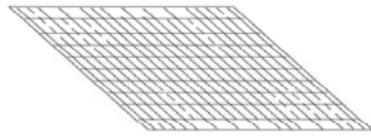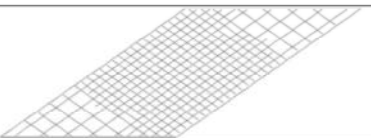
Table 1: Details of the analysed slabs [15]

Model No.	Angle of skew	Dimension	Volume of longitudinal steel	Volume of transverse steel	Steel arrangement
1	120	1945 x 2425	4.71	2.16	
2	45	2000 x 2970	2.058	1.718	
3	45	2000 x 2970			Details provided in reference [15]

Table 2: Mechanical properties of concrete for skew slabs used in the analysis [15]

	Measured Properties						Assumed Properties		
Model No.	E_C kg/cm^2	F_{cu} kg/cm^2	F_t kg/cm^2	E_s kg/cm^2	F_y kg/cm^2	ζ_y	A_1	A_2	A_3
1	2.925E5	450	29. 5	2.1E6	5000	0.0024	0.05	0.80	0.05
2	2.925E5	440	35	2.3E6	4600	0.002	0.30	0.75	0.65
3	2.925E5	440	35	2.3E6	4600	0.002	0.20	0.80	0.10

Table 3: Comparison between theoretical and experimental results for studied slabs.

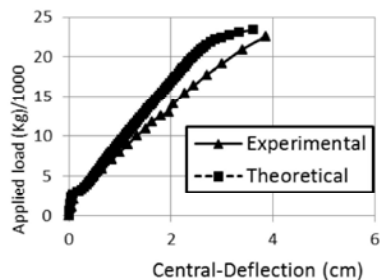| Model No	P_{Tc} / P_{Ec}	P_{Tf} / P_{Ef}	P_{Ty} / P_{Ey}	P_{Ts} / P_{Es}	A_{Tf} / A_{Ef}	Failure Type
1	1.00	0.99	1.00	1.00	1.06	Failure for all models were flexural,
2	1.03	0.93	0.92	0.85	1.05	similar to the experimental type of failure
3	0.99	0.99	1.06	1.07	0.98	

Fig. 2: Experimental and theoretical central deflection curves for model No. 1.
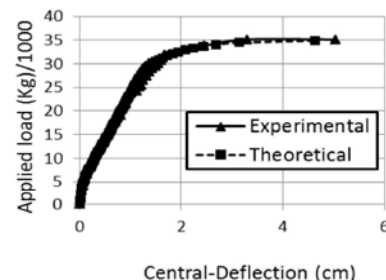

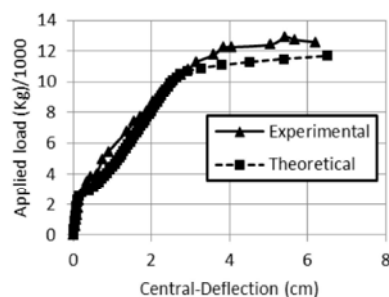Fig. 4: Experimental and theoretical central deflection curves for model No. 3.

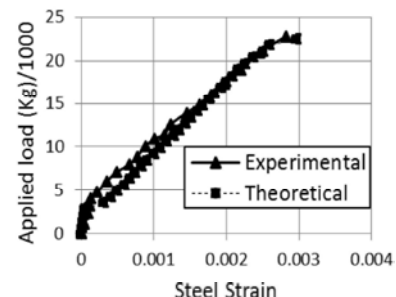Fig. 3: Experimental and theoretical central deflection curves for model No. 2.

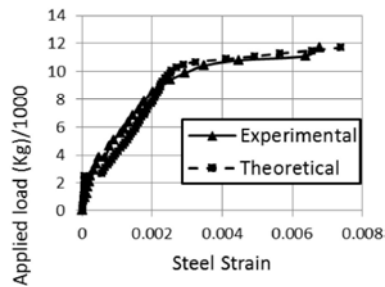Fig. 5: Experimental and theoretical longitudinal steel strain curves for model No. 1

Fig. 6: Experimental and theoretical longitudinal steel strain curves for model No. 2.
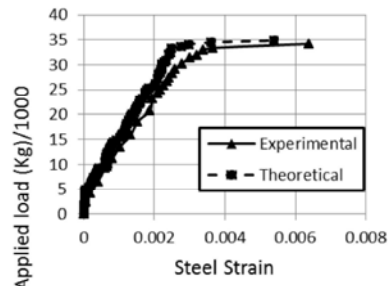

Fig. 7: Experimental and theoretical longitudinal steel strain curves for model No. 3.

1.06 of the experimental yield load for models 1, 2 and 3, respectively. The theoretical service load was 1.00, 0.85 and 1.07 of the experimental service load for models 1, 2 and 3, respectively. 1The theoretical failure load was 0.99, 0.93 and 0.99 of the experimental failure load for models 1, 2 and 3, respectively. The theoretical deflection at failure load was 1.06, 1.05 and 0.98 of the experimental deflection at failure for models 1, 2 and 3, respectively. Therefore, it can be concluded that the accuracy of the computer program (ANSYS) used in this study was verified by comparisons made against [15] experimental tests. Thus, the (ANSYS) software is capable of providing a good prediction of the overall behaviour of plane and ribbed reinforced concrete slabs failing in flexure.

Geometric Dimension and Steel Reinforcement of the Analysed Bridge Decks: The analysed bridge had a span of 12 m and a deck width of 8 m. The slab thickness was 300 mm. The ribs in each model had the same overall depth of 800 mm and breadth of 300 mm. The spacing between the ribs was kept constant in all analysed bridge decks, as shown in Fig. 8. Figs 9-10 present the area and the steel reinforcement arrangement for the longitudinal rib, respectively. The area and steel arrangement were kept constant for all models of different skew angles and different concrete grades.
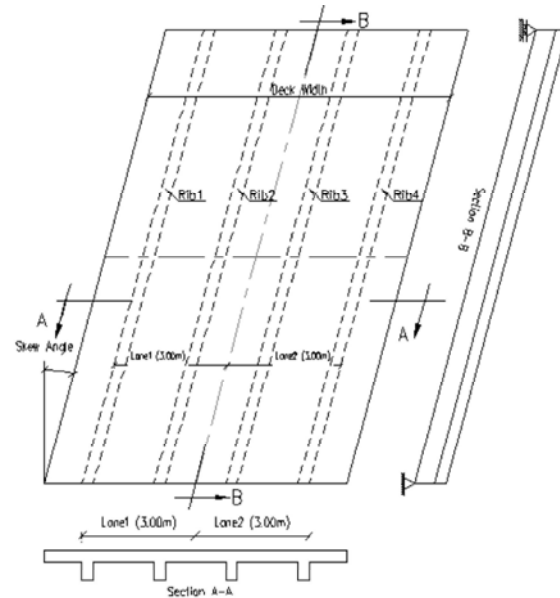

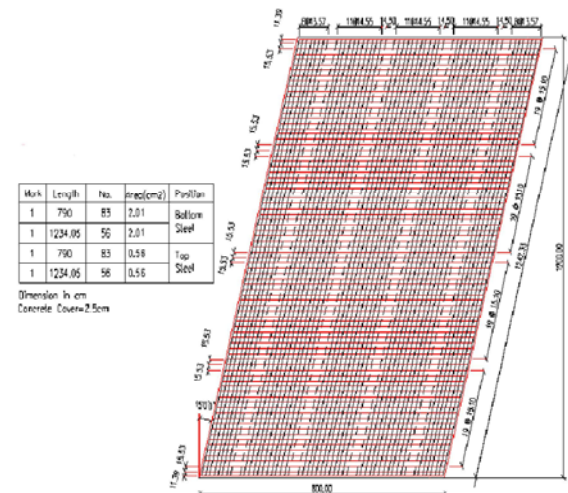Fig. 8: Layout and geometrical shape of skewed bridge decks.

Fig. 9: Longitudinal and transverse steel reinforcement of bridge deck in model No. 2.

Material Properties: Table 4 provides the properties of the materials used in all analysed models. All analysed bridge decks have the same Poisson`s ratio of 0.18 for concrete and 0.30 for steel reinforcement. High-strength concrete properties were used for modelling the bridge deck. The open and closed shear transfer coefficient was 0.40 and 0.80, respectively. The modulus of elasticity was calculated from equation (1) as follows:

$$E_c = \left(3320\sqrt{f_c} + 6900\right)\left(\gamma_c / 2300\right)^{1.5} \tag{1}$$

Table 4: Mechanical properties of concrete for skew slabs.

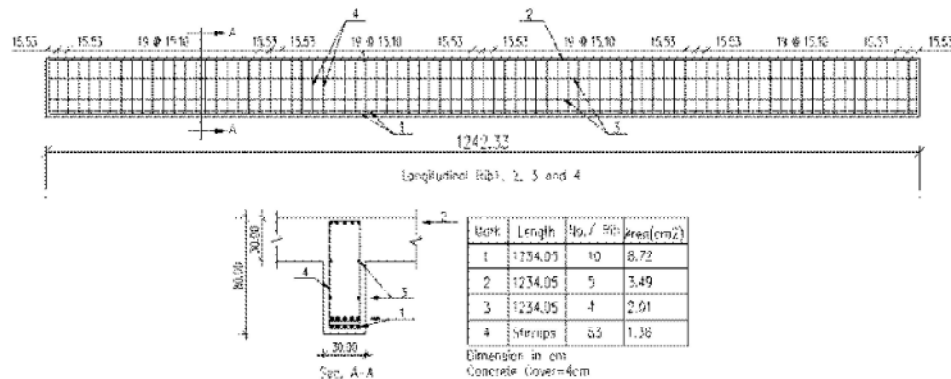| Group No.	Model No.	Fcu Kg/cm²	F$_t$ Kg/cm²	E$_c$ Kg/cm²	F$_y$ Kg/cm²	F$_{y(stirrups)}$ Kg/cm²	E$_S$ Kg/cm²
1,2	All models	700	50.2	392972	3600	2400	2100000

Fig. 10: Details of steel reinforcement for longitudinal ribs in model No. 2.

Where: fc is the cylinder compressive strength in MPa; and γc is the density of concrete in kg/m3. This equation is incorporated in the Canadian and New Zealand Standards [17].

The tensile strength was calculated from equation (2) as follows:

$$f_{ct} = {}^{0.60}\sqrt{f_c} \tag{2}$$

Where: fc is expressed in terms of MPa.

Loading and Boundary Conditions: The slab supports located at the edges were used for roller supports and the hinged supports were used to prevent translation perpendicular to the deck surface and translation parallel to the transverse direction of the deck. Loads consisted of a dead load and a live load. The dead load was comprised of self-weight and wearing coat. The live load was used as recommended by the Egyptian code of practice [16], as shown in Fig. 11.

Effect of Skew Angle on Cracking and Failure Load: The first crack was observed to be flexural for both the straight bridge (skew angle = 0°) and skewed models. It initiated at the bottom surface of the centre of the ribs in the pure bending zone. As the applied load increased, the cracks in the entire slab and in the ribs spread upwards to the compression zone. Furthermore, a few cracks initiated near the support because of the shear at the end of loading, as shown in Fig. 12. It was observed that an increase in the skew angle had a slight effect on the failure load. With an increase in the skew angle, the failure load
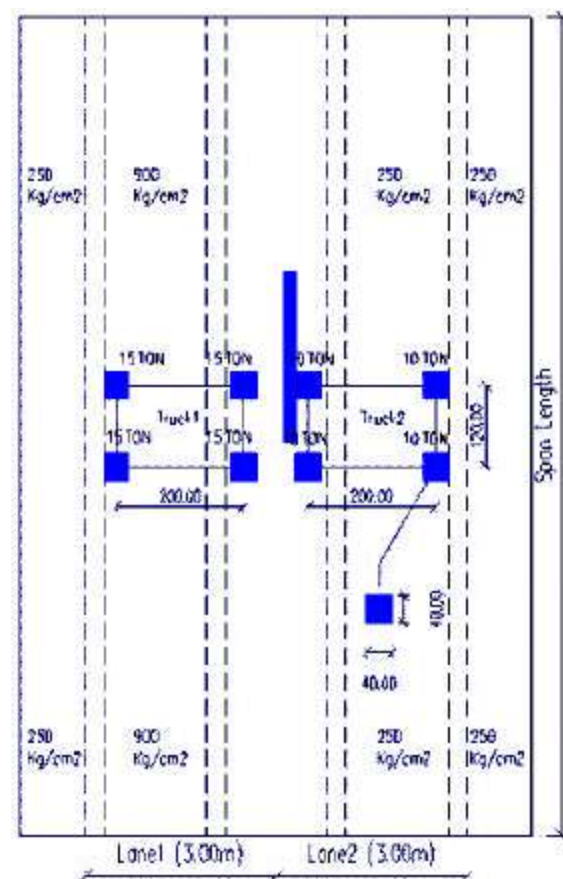

Fig. 11: Typical two-lane bridge deck loaded with two trucks [16].

decreased. The ratio of decrease for the ultimate load was small for a skew angle of 15° while the ratio of decrease for the ultimate load was considerable for skew angles greater
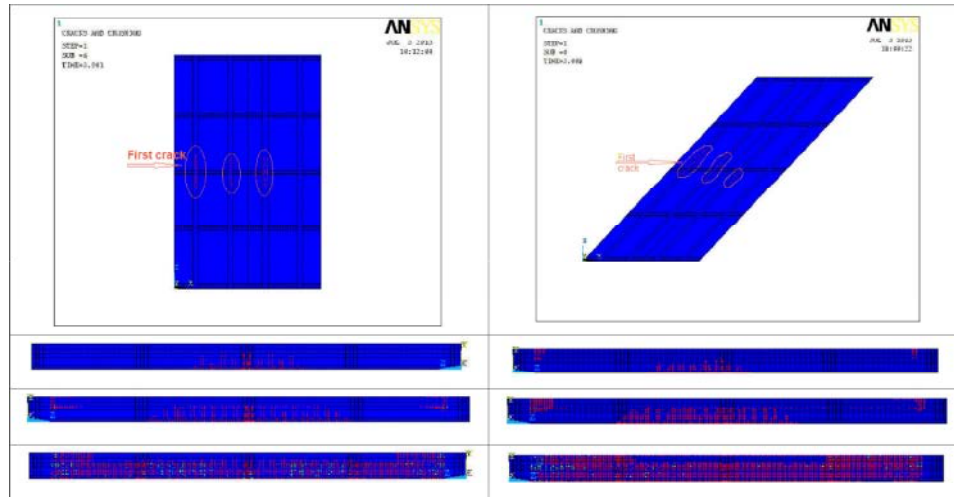
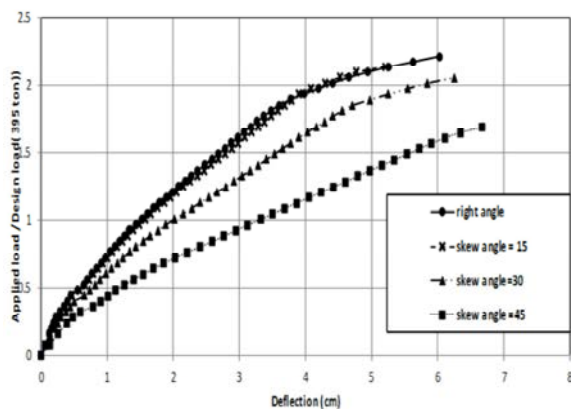Fig. 12: Pattern of cracks in models one and four.

Fig. 13: Load vs. Central deflection curves for different angles of skew.

than 15°. Failure occurred due to yielding of the tension reinforcement in the middle of the ribs for all decks. It was observed that the final mode of failure for all bridge decks was tension flexural failure.

Effect of Skew Angle on Deflection: Fig. 13 provides load vs. deflection curves for different skew angles at longitudinal rib 1. It was observed that the maximum central deflection increased when the skew angle increased. The maximum central deflection values for skew angles 15°, 30° and 45° at service load were 1.05, 1.3 and 1.80 of the maximum central deflections for a straight angled slab (reference slab), respectively. The load vs. deflection curve for decks with a skew angle of 15° is similar to the load vs. deflection curve for a straight angled slab.

Effect of Skew Angle on Soffit and Top Steel Stresses: With an increase in the skew angle, the stresses in the ribs differed significantly compared to those in a straight bridge deck. Fig. 14 provides load vs. steel stress curves for different skew angles at longitudinal rib 1. When the skew angle of the bridge decks decreased, the rigidity of the plate increased and the strength of the overall structure improved. It can be observed from these curves that at the centre of longitudinal rib number 1, the steel yielded at 1.00, 1.00 and 0.90 of the yield load of the reference bridge deck for skew angles of 15°, 30° and 45°, respectively. It can be observed that there is no marked difference between the stresses of the bridge deck with a skew angle of 15° and the straight bridge deck. The top steel (compression zone) carried stresses that were minor compared to the bottom stresses. Fig. 15 provides load vs. top compressive steel stress curves for different skew angles at the mid-span of longitudinal rib 1. It can be observed that the top compressive strength increases with an increase in the skew angle. There is no difference between the deck with a skew angle of 15° and the straight deck and this result confirmed the load-soffit steel stress curves and load-deflection curves mentioned previously.

Effect of Skew Angle on Top Surface Compression Principal Concrete Strain: The principal concrete strains at the top surface of the mid-span of longitudinal rib 1 for different skew angles are provided in Fig. 16. The maximum concrete strain occurred in the mid-span of rib 1 and rib 2 for the straight and skewed bridge, respectively. The concrete strain at the top   surface
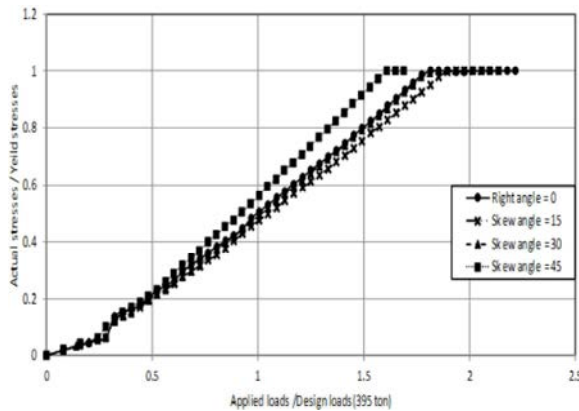
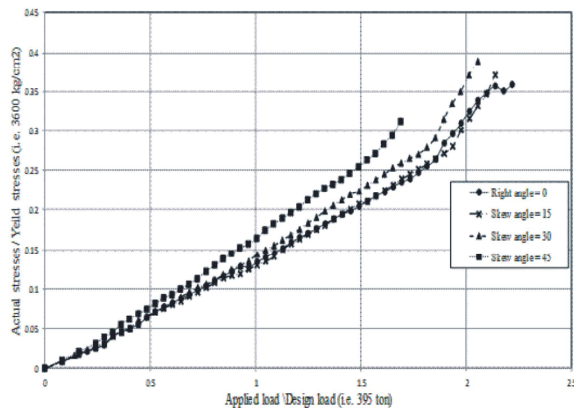Fig. 14: Applied loads/Design loads vs. Actual stress/Yield stress curves for different skew angles

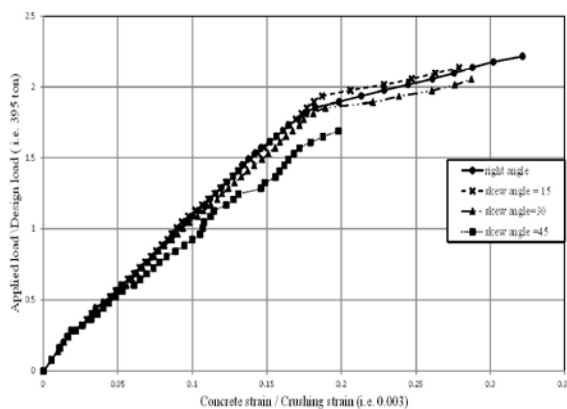Fig. 15: Load vs. Top compressive steel stress curves for different skew angles.

Fig. 16: Load vs. Principal concrete strain curves for decks with different skew angles.

increased with an increase in the skew angle. The concrete strain values are 1.00, 1.10 and 1.30 of the concrete strain for the reference deck at service load
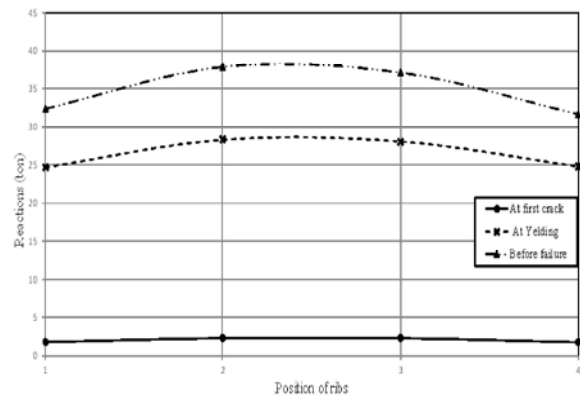

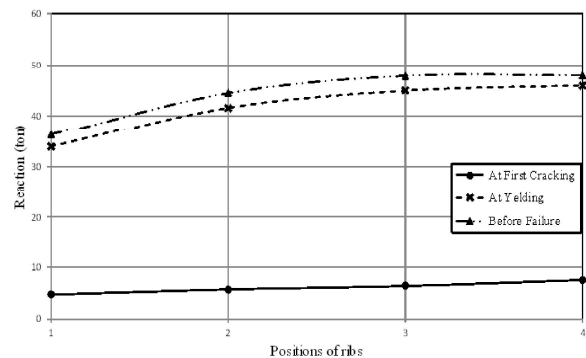Fig. 17: Support reaction at each rib for straight bridge decks.

Fig. 18: Support reaction at each rib for decks with a skew angle of 45°.

(0.8 of the yielding load) for decks with skew angles of 15°, 30° and 45°, respectively. The concrete strain for a deck with a skew angle of 15° is the same as the concrete strain for a straight bridge deck.

Effect of Skew Angle on the Support Reactions: To study the effect of skew angle on the support reactions, a symmetrical loading case was considered. When the bridge is skewed, the distribution of reactions and shears becomes more complicated. Figs 17-18 provide the distribution of reaction forces at cracking, yielding and before failure for decks with skew angles of 0° and 45°, respectively. The presence of skew causes a high concentration of reactions at the ribs closest to the obtuse corner and reduces the concentration of reactions in the girder closest to the acute corner as well as in the interior ribs. The bearings below the end of the bridge decks with an obtuse angle indicate the largest reaction forces. When the skew angle is reduced, the reaction force is decreased. The reaction force at rib 1 was nearly

equal to the reaction forces at rib 4. Similarly, reaction forces were nearly equal for rib 2 and 3 for the straight bridge deck. For decks with a skew angle of 45°, the reaction forces increased as we moved towards the obtuse angle. The reaction forces at rib 1 in the acute corner were 0.63, 0.74 and 0.76 of the reaction force at rib 4, which was similar to the reaction forces for cracking, yielding and before failure, respectively, at the obtuse corner. Thus, it can be concluded that the bearing in RC slab bridges with skew should be selected carefully by considering the variation in reaction forces.

Effect of Concrete Grade on Cracking Load and Failure Load: The cracking load increased with an increase in the compressive strength. The cracking load values of the straight bridge with compressive strengths of 500, 600, 700, 800 and 900 kg/cm² were 110%, 115%, 115%, 120% and 130%, respectively, of the cracking load of a deck with a compressive strength of 400 kg/cm². The cracking load values for a bridge deck with a skew angle of 30° with compressive strengths of 500, 600, 700, 800 and 900 kg/cm² were 120%, 120%, 130%, 130% and 150%, respectively, of the cracking load of a deck with a compressive strength of 400 kg/cm². The first crack was observed to be flexural for both the straight bridge (skew angle = 0°) and the skewed bridge (skew angle = 30°). The crack pattern and failure shape are similar to the control slab. The failure load increased when the compressive strength increased. An increase in the compressive strength from 400 to 900 kg/cm² led to an increase in the failure load of approximately 30% and 50 % for decks with skew angles of 0° and 30°, respectively. The failure load values for straight decks with compressive strengths of 500, 600, 700, 800 and 900 kg/cm² were 100%, 120%, 125%, 130% and 130%, respectively, of the ultimate load for a deck with a compressive strength of 400 kg/cm². For decks with skew angles of 30°, the ultimate loads were 115%, 120% and 130%, 140% and 150%, respectively, of the ultimate load for a deck with a compressive strength of 400 kg/cm².

Effect of Concrete Grade on Deflection: Figs 19-20 provide load vs. deflection curves for decks with different compressive strength values of 400, 500, 600, 700, 800 and 900 kg/cm² for straight decks and decks with a skew angle of 30°. As recommended by ACI435R-95, the deflection limit of span/480 was reached at 1.29, 1.35, 1.37, 1.45, 1.47 and 1.49 of the design load for the right bridge decks with compressive strengths of 400, 500, 600, 700, 800 and 900 kg/cm², respectively. For a skew angle of 30°, the
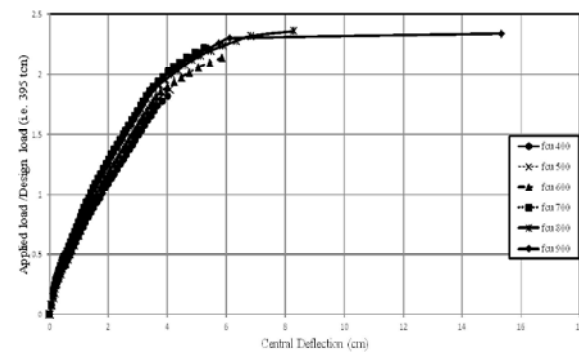

Fig. 19: Load vs. Central deflection curves for straight decks with different compressive strengths at longitudinal rib No. 1.
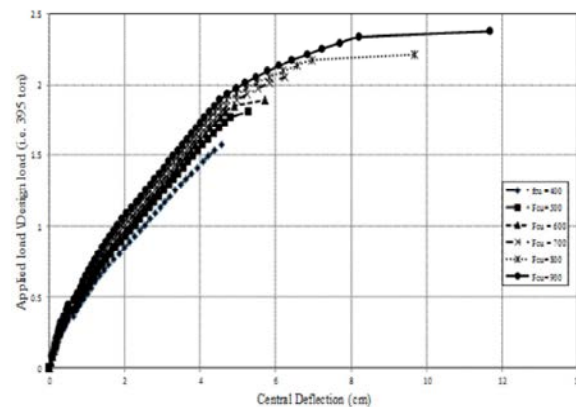

Fig. 20: Load vs. Central deflection curves for 30° decks with different compressive strengths at longitudinal rib No.1.

deflection limits were reached at 1.13, 1.21, 1.25, 1.29, 1.33 and 1.37 of the design load for bridge decks with compressive strengths of 400, 500, 600, 700, 800 and 900 kg/cm², respectively. The maximum central deflection for straight decks with compressive strengths of 500, 600, 700,800 and 900 kg/cm² was 100%, 100%, 90%, 90% and 90% of the maximum central deflection for a deck with compressive strength of 400 kg/cm², respectively, at service load. For a deck with a skew angle of 30°, the maximum central deflection was nearly equal to the maximum central deflection of a deck with a compressive strength of 400 kg/cm² at service load. The maximum central deflection occurred near rib 1, which was loaded by the heavy truck. Increasing the compressive strength had a slight effect on the deflection for both straight and skewed bridge decks. The ratio of decreasing the deflection was approximately 10% when the compressive strength increased from 400 to 900 kg/cm² for straight bridge decks.
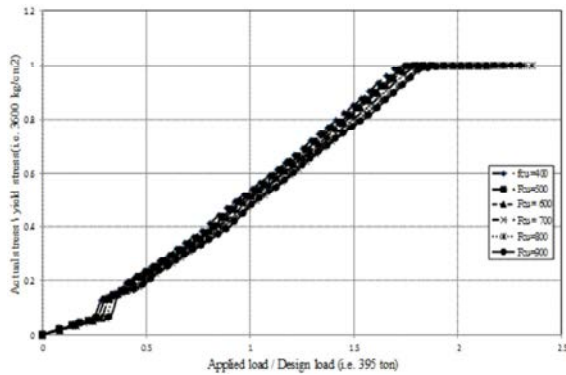
Fig. 21: Load vs. Soffit steel stress curves for straight decks with different compressive strengths at longitudinal rib no.
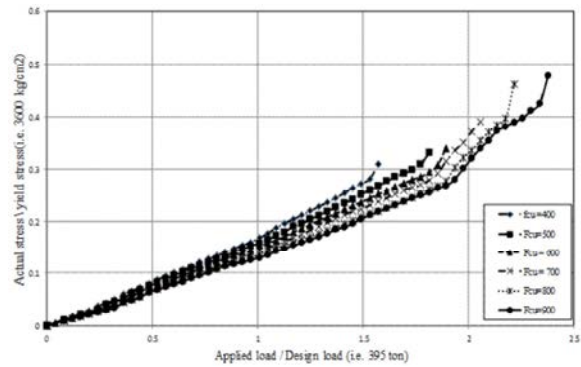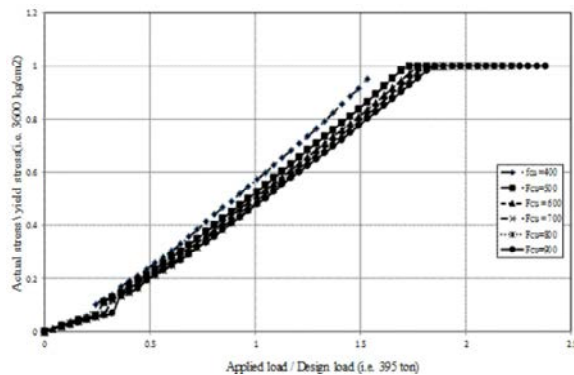

Fig. 22: Load vs. Soffit steel stress curves for 30° decks with different compressive strengths at longitudinal rib No. 1.
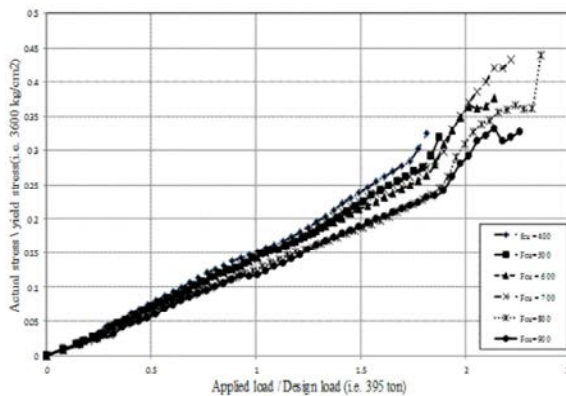

Fig. 23: Load vs. Top steel stress curves for decks with skew angle of 0° for different compressive strengths.

Effect of Concrete Grade on Soffit and Top Steel Stresses: Figs 21-22 provide load vs. stress curves for decks with different compressive strengths and skew angles of 0° and 30°. For straight bridge decks, the steel

Fig. 24: Load vs. Soffit steel stress curves for decks with skew angle of 30° for different compressive strengths.

reinforcement first yielded in the middle of rib 1 at 1.77, 1.80, 1.82, 1.82, 1.88 and 1.94 of the design load for decks with compressive strengths of 400, 500, 600, 700, 800 and 900 kg/cm^2, respectively. For a skew angle of 30°, the steel reinforcement yielded at 1.57, 1.73, 1.81, 1.85, 1.85 and 1.85 of the design load for different concrete grades, respectively. Increasing the compressive strength had insignificant effects on the steel stresses for both straight and skewed bridge decks. The ratio of increasing the yielding load was approximately 10% for straight bridge decks when the compressive strength increased from 400 to 900 kg/cm^2. For a skewed bridge with a skew angle of 30°, the ratio of increasing the yielding load was approximately 20% for decks with a compressive strength of 900 kg/cm^2. The top steel stress at the mid-span of the longitudinal ribs for the straight bridge deck carried stresses of approximately 0.32, 0.32, 0.38, 0.43, 0.44 and 0.70 of the yield stress at failure load for compressive strengths of 400, 500, 600, 700, 800 and 900 kg/cm^2, respectively. For a deck with a skew angle of 30°, the top steel stresses were 0.31, 0.33, 0.34, 0.39, 0.46 and 0.48, respectively. Figs. (23-24) provide top steel stresses for deck bridges with skew angles of 0° and 30°.

Effect of Concrete Grade on the Top Surface Compression Principal Concrete Strain: The principal concrete strains at the top surface of the longitudinal ribs are provided in Figs 25-26. The maximum concrete strain occurred at the mid-span of each longitudinal rib. It can be observed from the curves that the general behaviour is similar to the overall behaviour of the bridge deck, as shown in load-deflection curves. The principal concrete strain for straight bridge decks with compressive strengths of 400, 500, 600, 700, 800 and 900 kg/cm2 was 0.23, 0.23, 0.31, 0.31, 0.36 and 0.57 of the crushing strain at
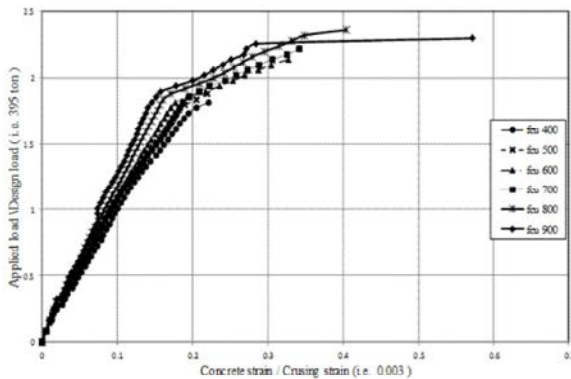
Fig. 25: Load vs. Principal concrete strain for straight decks with different compressive strengths.
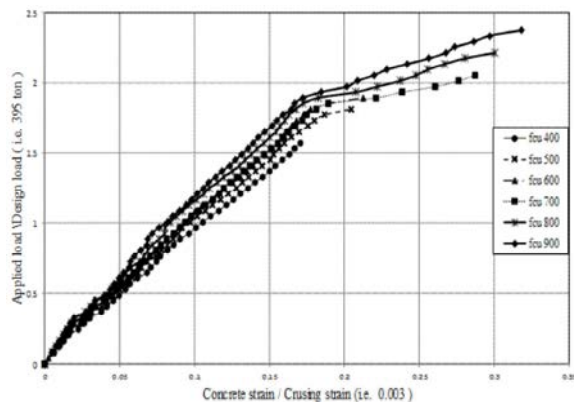

Fig. 26: Load vs. Principal concrete strain curves for 30° decks with different compressive strengths.

failure, respectively. The principal concrete strain for decks with a 30° skew angle and compressive strengths of 400, 500, 600, 700, 800 and 900 kg/cm^2 were 0.22, 0.25, 0.27, 0.28, 0.39 and 0.52 of the crushing strain at failure, respectively.

Effect of Concrete Grade on Ductility: The ductility index for the straight bridge deck (skew angle = 0°) with compressive strengths of 400, 500, 600, 700, 800 and 900 kg/cm^2 was 1.05, 1.10, 1.30, 1.30, 1.30 and 1.30, respectively. The ductility index of bridge decks with a skew angle of 30° and compressive strengths of 400, 500, 600, 700, 800 and 900 kg/cm^2 was 1.0, 1.10, 1.10, 1.20, 1.30 and 1.40, respectively. Because a value of 3 for the ductility index represents an acceptable lower bound for the ductile behaviour of flexural members as recommended by several researchers, the value of the ductility index for the considered models of this group was small. It can be observed that the ductility index of bridge decks with a skew angle of 0° and compressive strengths of 500, 600, 700, 800 and 900 kg/cm^2 were 1.10, 1.20, 1.30, 1.30 and 1.30,

respectively, of the ductility index for decks with a compressive strength of 400 kg/cm^2. The ductility index for bridge decks with a skew angle of 30° and concrete compressive strengths of 500, 600, 700, 800 and 900 kg/cm^2 were 1.10, 1.10, 1.20, 1.30 and 1.40, respectively.

DISCUSSION

An increase in skew angle up to approximately 30° had no effect on the cracking load. The cracking load for decks with a skew angle of 45° was less compared to that for a skew angle of 30°, which is because the span of the bridge deck was 40% greater than the span of the straight bridge deck. The load for the first crack for skew angles of 15° and 30° was equal to the cracking load of the reference slab; however, for a skew angle of 45°, the load was 0.875 of the cracking load of the reference bridge deck, as presented in Fig. 27. The increase in skew angle had a slight effect on the failure load. When the skew angle increased, the failure load decreased. The ratio of decrease for the ultimate load was small for a skew angle of 15° while the ratio of decrease for the ultimate load was considerable for skew angles greater than 15°. This result is consistent with AASHTO [20], which suggests that bridges with a skew angle less than or equal to 20° can be designed as a typical bridge at straight angles with no modifications. However, if the skew angle exceeds 20°, AASHTO [20] suggests the use of an alternate superstructure configuration. The ultimate load values for decks with angles of 15°, 30° and 45° were 0.96, 0.93 and 0.76, respectively, of the ultimate load for straight bridge decks, as presented in Fig. 28.

With an increase in the skew angle, the stresses in the ribs differed significantly compared to those in a straight bridge deck. With a decrease in the skew angle of the bridge decks, the rigidity of the plate increased and the strength of the overall structure improved. At the centre of longitudinal rib number (1), the steel yielded at 0.99, 0.99 and 0.84 of the yield load for the reference bridge deck for skew angles of 15°, 30° and 45°, respectively, as shown in Fig. 29.

The different concrete grades play a significant role in enhancing the skew slab behaviour. The cracking load increases as the compressive strength increases. When the concrete compressive strength of the slab is increased from 400 to 900 kg/cm^2, an increase in the cracking load is achieved at approximately 30% for straight bridge decks and approximately 50% for decks with a skew angle of 30°. Figs 30-31 provide the cracking load for decks with different compressive strengths and skew angles of 0° and 30°. The ultimate load increases as the compressive
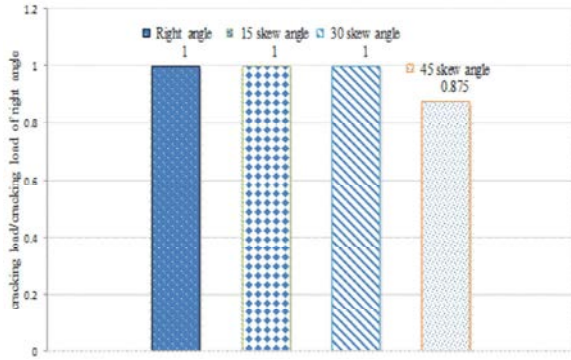
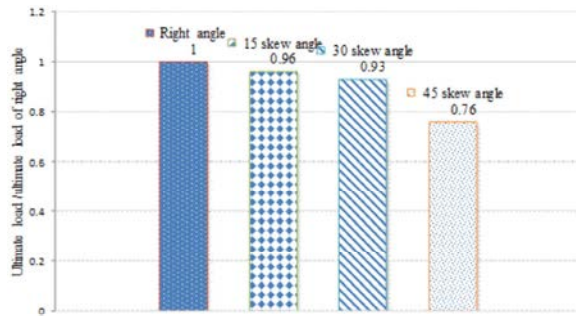Fig. 27: Cracking load for different skew angles.

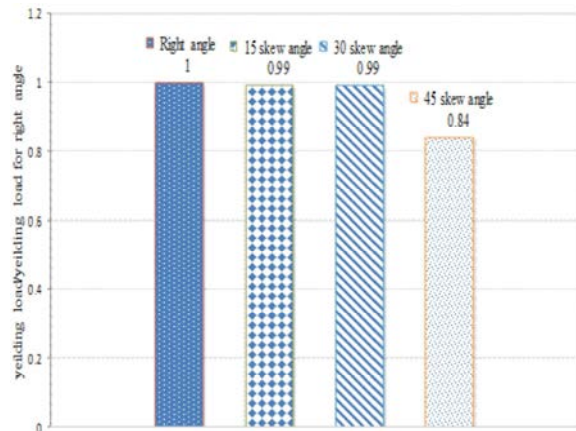

Fig. 28: Failure load for different skew angles.

Fig. 29: Yielding load for different skew angles.

strength increases. Increasing the compressive strength from 400 kg/cm² to 900 kg/cm² leads to an increase in the ultimate load of approximately 30% and 50 % for decks with skew angles of 0° and 30°, respectively. Figs 32-33 provide the ratio of increasing the ultimate load at different compressive strengths for straight and skewed bridge decks. The effect of compressive strength is more effective on skewed bridge decks than straight bridge decks. Table 5 summarises the results of the analysed models. The final mode of failure for straight and skewed bridge decks (skew angles = 0° and 30°) with different
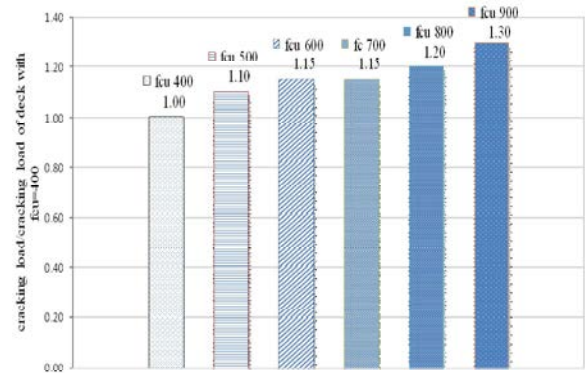

Fig. 30: Cracking load/cracking load of deck with f_{cu} = 400 kg/cm² for right angle for different compressive strengths.
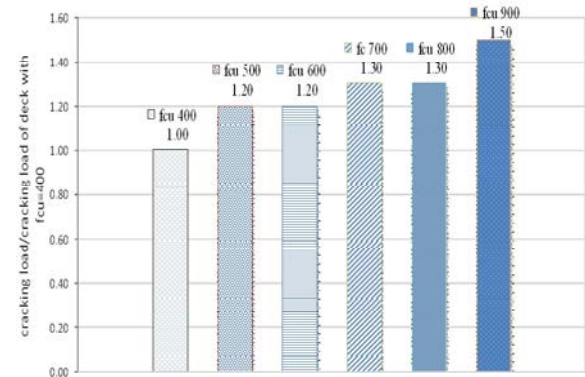

Fig. 31: Cracking load/cracking load of deck with f_{cu} = 400 kg/cm² for 30° angle for different compressive strengths.
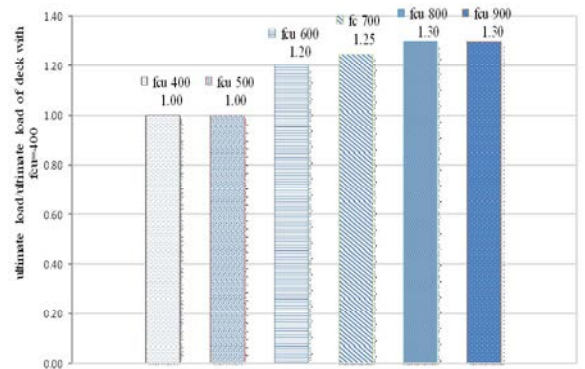

Fig. 32: Ultimate load/ultimate load of deck with f_{cu} = 400 kg/cm² for right angle for different compressive strengths.

compressive strengths (400 kg/cm² to 900 kg/cm²) was tension flexural failure caused by yielding of the tension reinforcement at the mid–span of rib(1), which was loaded by a 60 ton truck.

Table 5: Summary of the main results for group C.

| Model	Skew angle	Grade of concrete	P_c / P_{cw}	P_y / P_{yw}	P_f / P_{fw}	Deflection			$\varepsilon /\varepsilon_w$	μ_d /μ_{dw}	Failure type
						δ_c /δ_{cw}	δ_s /δ_{sw}	δ_y /δ_{yw}			
D1	0°	400	1.00	1.00	1.00	1.0	1.00	1.00	1.00	1.0	Ductile failure
D2		500	1.10	1.00	1.00	1.0	1.00	1.00	0.90	1.05	
D3		600	1.15	1.05	1.20	1.0	1.00	1.00	0.90	1.40	
D4		700	1.15	1.05	1.25	1.0	0.90	0.90	0.90	1.40	
D5		800	1.20	1.10	1.30	1.0	0.90	0.90	0.90	1.70	
D6		900	1.30	1.10	1.30	1.0	0.90	0.90	0.90	1.70	
D7	30°	400	1.00	1.00	1.00	1.0	1.00	1.00	1.00	1.00	Ductile failure
D8		500	1.20	1.10	1.15	1.0	1.00	1.00	1.00	1.05	
D9		600	1.20	1.20	1.20	1.0	1.00	1.00	1.00	1.20	
D10		700	1.30	1.20	1.30	1.0	1.00	1.00	1.00	1.30	
D11		800	1.30	1.20	1.40	1.0	1.00	1.00	1.00	1.50	
D12		900	1.50	1.20	1.50	1.0	1.00	1.00	1.00	1.90	
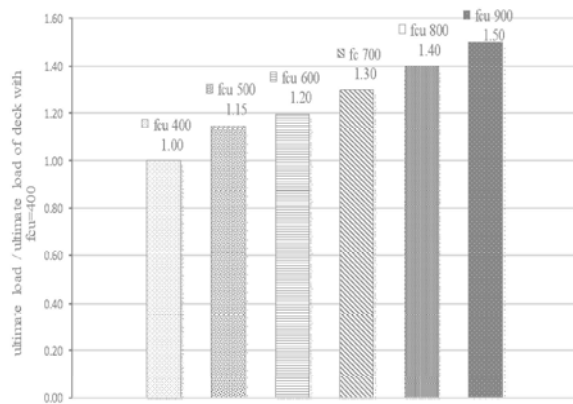
Fig. 33: Ultimate load/ultimate load for decks with $f_{cu}=$ 400 kg/cm^2 for 30° angle for different compressive strengths.
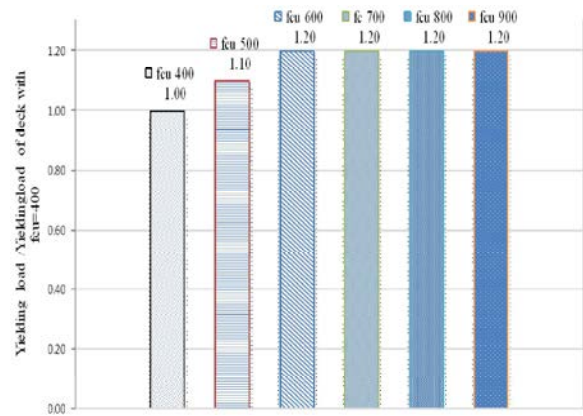
Fig. 34: Yielding load for decks with different compressive strengths with skew angle of 0°.
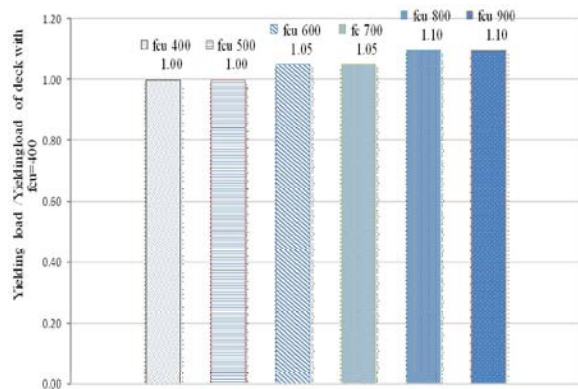

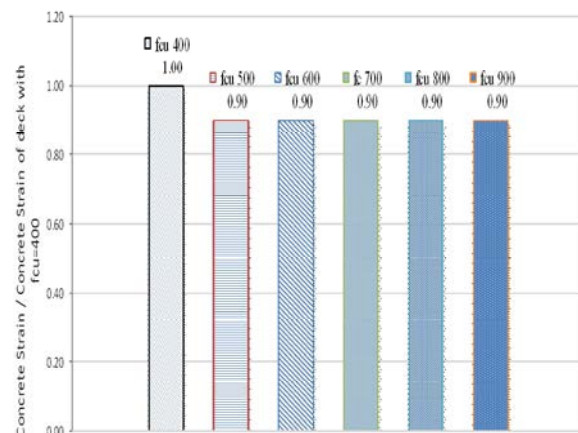Fig. 35: Yielding load for decks with different compressive strengths with skew angle of 30°.

Fig. 36: Principal concrete strain for decks with different compressive strengths with skew angle of 0°.

The maximum central deflection occurs near rib (1), which is loaded by the heavy truck. Increasing the compressive strength had a slight effect on the deflection for both straight and skewed bridge decks. The ratio of decreasing the deflection was approximately 10% when the compressive strength increased from 400 to 900
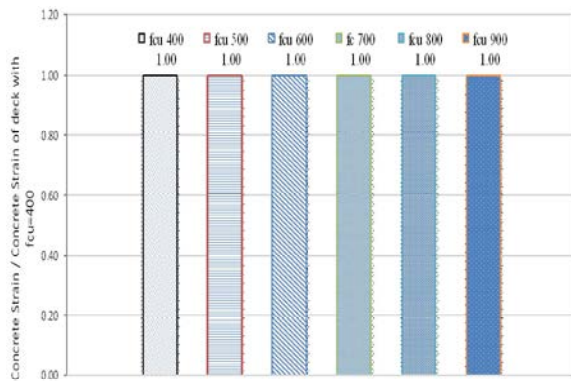
Fig. 37: Principal concrete strain for decks with different compressive strengths with skew angle of 30°.
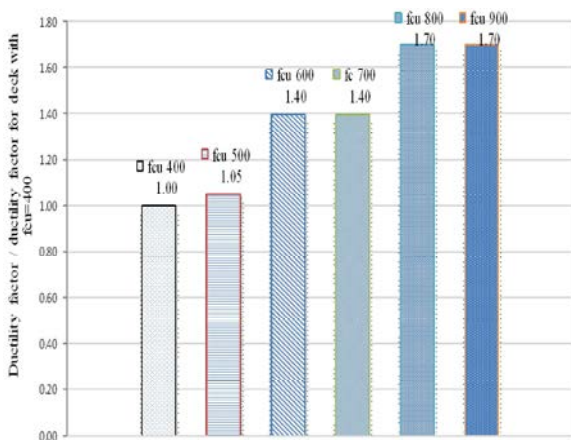

Fig. 38: Ductility factor for decks with different compressive strengths with skew angle of 0°.
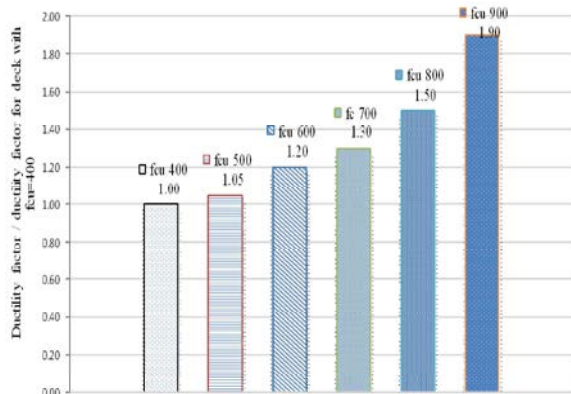

Fig. 39: Ductility factor for decks with different compressive strengths with skew angle of 30°.

kg/cm2 for both straight and skewed bridge decks. The deflection for decks with a skew angle of 30° is nearly equal. For skewed bridges with a skew angle of 30°, the

ratio of increase in the yielding load was approximately 20% for decks with a compressive strength of 900 kg/cm^2. Figs. 34-35 provide the yielding load for decks with different compressive strengths.

Figs 36-37 provide the principal concrete strains at the top surface of the mid-span of longitudinal rib 1 for different skew angles at service load (0.80 of the yielding load). The compressive strength has an insignificant effect on the principal concrete strain. The concrete strain values were nearly equal for both straight and skewed bridge decks with different compressive strengths. The principal concrete strain was reduced by 10% due to increasing the compressive strength from 400 to 900 kg/cm^2 for a straight bridge deck. However, the principal concrete strain was equal for skewed bridge decks. Fig. 38-39 provide the influence of concrete compressive strength on ductility. It can be observed that the ductility index of bridge decks with a skew angle of 0° for compressive strengths of 400, 500, 600, 700, 800 and 900 kg/cm^2 were 1.0, 1.05, 1.40, 1.40, 1.70 and 1.70, respectively. The ductility index for bridge decks with a skew angle of 30° for concrete compressive strengths of 400, 500, 600, 700, 800 and 900 kg/cm^2 were 1.0, 1.05, 1.20, 1.30, 1.50 and 1.90, respectively. It can be concluded that the deflection ductility index increases with an increase in the concrete compressive strength for both straight and skewed bridge decks.

CONCLUSIONS

Based on the results of the finite element analysis and the comparisons of skew bridges with straight bridges, the following points can be concluded.

- Skew bridges exhibit greater displacements for the same loadings and boundary conditions compared to those of straight bridges.
- As the skew angle increased, the deflection increased and the failure load decreased.
- The results of this study agree well with the AASHTO standard specifications in recommending that bridges with skew angles less than or equal to 20° should be designed as straight bridges. However, it is preferable to perform three-dimensional finite element analysis for skewed bridge decks.
- Increasing the compressive strength has a considerable effect on the cracking load, ultimate load and ductility factor. However, it has an insignificant effect on deflection, steel stresses and principal concrete strain.

- As the compressive strength increased, the cracking, ultimate load, yielding load and ductility increased. However, the deflection and concrete strain decreased for both straight and skewed bridge decks.
- With an increase in the skew angle, the stresses in the skewed bridge deck differ significantly compared to those in a straight bridge deck.
- It can be concluded that the deflection ductility index increases with an increase in the concrete compressive strength for both straight and skewed bridge decks.
- The bearing in reinforced concrete skewed slab bridges should be selected carefully by considering the variation in the reaction forces.

Notations:

Av   = Area of horizontal reinforcement within distance of s, in.2
Avf = Area of total reinforcement (sum of areas of vertical web
Md   = Ductility factor
Δy   = Deflections at yielding
Md   = Ductility factor
A1   = Open shear transfer coefficient
A2   = Closed shear transfer coefficient
A3   = Tensile crack factor
Pcr = Cracking load
PTc = Theoretical cracking load
PEc = Experimental cracking load
PTf = Theoretical failure load
PEf = Experimental failure load
PTy = Theoretical yielding load
PEy = Experimental yielding load
PTs = Theoretical service load
PEs = Experimental service load
δTf   = Theoretical deflection at failure
δEf   = Experimental deflection at failure
Pf   = Failure load
Pc w. = Cracking load of reference deck
Py w = Yielding load of reference deck
Pf w = Failure load of reference deck
Ac   = Deflection at cracking
Ac ref = Deflection at cracking of reference deck
As   = Deflection at 0.8 of the design load
As w = Deflection at 0.8 of the design load of reference deck
Ay ref = Deflection at yielding of reference deck
Δ = Concrete principal strain at 0.80 yielding load

Δw   = Concrete principal strain at 0.80 of yielding load of reference deck.
µd ref = Ductility factor for reference deck.

REFERENCES

1. Sk. Md. Nizamud-Doulah and Ahsanul Kabir, 2001. Non-Linear Finite Element Analysis of Reinforced Concrete Rectangular and Skew Slabs. Journal of Civil Engineering. The Institution of Engineers, Bangladesh, 29(1): 1-16.
2. Madhu Sharma, 2011. Finite Element Modelling of Reinforced Cement Concrete Skew Slab. Department of Civil Engineering, Thapar University, Patiala, INDIA (July-2011).
3. Chen, W.F. and E.C. Ting, 1980. Constitutive Models for Concrete Structures. Jnl. ASCE, 106(1): 1-19.
4. Gupta, A.K. and H. Akbar, 1984. Cracking in Reinforced Concrete Analysis. Jnl. Struct. Eng. Div. ASCE, 110(8): 1735-1746.
5. Hu, H.T. and W.C. Schonobrich, 1990. Non-Linear Analysis of Cracked Reinforced Concrete. Jnl. of ACI (Struct.), 87(2): 199-207.
6. Gopalakrishnan, S., S.V.K. Mohan Rao and T.V.S.R. Appa Rao, 1993. Non-Linear Analysis of Reinforced Concrete Hyperboloid cooling Towers-1– Material Model, Finite Element Model and Validation Computers and Structures. 49(6): 913-921.
7. Gupta, T. and A. Misra, 2007. Effect on Support Reactions of T Beam Skew Bridge Decks. ARPN Journal of Engineering and Applied Sciences, 2(1): 1-8.
8. Hambly, E.C., 1976. Bridge Deck Behaviour. Chapman and Hall, London.
9. Ansuman Kar, Vikash Khatri, P.R. Maiti and P.K. Singh, 2012."Study on Effect of Skew Angle in Skew. International Journal of Engineering Research and Development, 2(12): 13-18.
10. Ansuman Kar, 2012. Analysis of skew bridges using computational methods. M. Tech Dissertation, Department of Civil Engineering, Institute of Technology, Banaras Hindu University, Varanasi.
11. Kassahun K. Minalu, 2010. Finite Element Modelling of Skew Slab-Girder Bridges" M.Sc.D. Thesis, Faculty of Civil Engineering and Geosciences, Technical University of Delft.
12. Ibrahim S. and I. Harba, 2011. Effect of Skew Angle on Behaviour of Simply Supported R. C. T-Beam Bridge Decks. ARPN Journal of Engineering and Applied Sciences, 6(8):1-14.

13. AASHTO, 2003. Standard Specifications for Highway Bridges. Washington, D.C.

14. Menassa, C., M. Mabsout, K. Tarhini and G. Frederick, 2007. Influence of Skew Angle on Reinforced Concrete Slab Bridges. Journal of Bridge Engineering, ASCE, 12(2): 205-2013.

15. El-Hafez, L.M., 1986. Direct Design of Reinforced Concrete Skew Slabs. Ph. D. Thesis, Dep. of Civil Eng. University of Glasgow.

16. Egyptian code of practice, ECP 201-2011.

17. Vijaya B. Rangan, 1998. High-Performance, High Strength Concrete Design Recommendations. Curtin University of Technology, Perth, Western Australia.

18. Rashid, M. A. and M. A. Mansur, 2005. Reinforced High-Strength Concrete Beams in Flexure. ACI Structural Journal, 102(3):462-471.